Glycobiology vol. 20 no. 7 pp. 883–894, 2010
doi:10.1093/glycob/cwq046
Advance Access publication on March 30, 2010

NMR characterization and molecular modeling of fucoidan showing the importance of oligosaccharide branching in its anticomplementary activity

Marie-Jeanne Clément[4], Bérangère Tissot[3,2], Lionel Chevolot[6], Elisabeth Adjadj[4], Yuguo Du[5], Patrick A Curmi[4], and Régis Daniel[3,1]

[3]CNRS UMR 8587, Laboratoire Analyse et Environnement and [4]INSERM/UEVE U829, Laboratoire Structure et Activité des Biomolécules Normales et Pathologiques, Université d'Évry Val d'Essonne, rue du Père Jarlan, 91025 Évry Cedex, France, [5]Research Center for Eco-Environmental Sciences, Chinese Academy of Sciences, PO Box 2871, Beijing 100085, PR China, and [6]UPS-CNRS 2561, 16 rue A. Aron, 97300 Cayenne, French Guiana, France

Received on November 13, 2009; revised on March 19, 2010; accepted on March 19, 2010

Fucoidan is a potent inhibitor of the human complement system whose activity is mediated through interactions with certain proteins belonging to the classical pathway, particularly the protein C4. Branched fucoidan oligosaccharides displayed a higher anticomplementary activity as compared to linear structures. Nuclear magnetic resonance (NMR) characterization of the branched oligosaccharides and saturation transfer difference-NMR experiment of the interaction with the protein C4 allowed the identification of the glycan residues in close contact with the target protein. Transferred nuclear Overhauser effect spectroscopy experiment and molecular modeling of fucoidan oligosaccharides indicated that the presence of side chains reduces the flexibility of the oligosaccharide backbone, which thus adopts a conformation which is very close to the one recognized by the protein C4. Together, these results suggest that branching of fucoidan oligosaccharides, determining their conformational state, has a major impact on their anticomplementary activity.

Keywords: complement system/fucoidan/molecular modeling/protein C4/STD-NMR

Introduction

Algal fucoidan is a sulfated polysaccharide extracted from brown algae (Usov and Bilan 2009). Because of its biological activities on mammalian systems, this polymer has raised increasing interest over the past decades (Lake et al. 2006; Boisson-Vidal et al. 2007; Lee et al. 2008). One of its known activities is its potent inhibitory effect on human complement system (Tissot and Daniel 2003). This property is of major interest given the involvement of complement in numerous pathological processes and the strong demand for efficient complement inhibitors. Complement is an important part of the human immune system being a major effector of innate immunity and playing an essential role in host defense against pathogens. However, inappropriate activation of complement has been recognized to play a key role in a variety of pathologies (Speth et al. 1999; Tedesco et al. 1999), including hyper-acute graft rejection in xenotransplantation (Winkler 2001), reperfusion injuries and more recently in neurodegenerating processes (Bergamaschini et al. 2001). Encompassing nearly 30 plasma and membrane proteins, complement is activated through three major ways: the classical pathway depending on antigen-bound antibody recognition and including the proteins C1q, C1r, C1s, C2, C4 and C1Inh, the lectin pathway involving the mannose-binding lectin MBL—this pathway merges with the classical pathway at the C4 activation step—and the alternative pathway triggered by contact on microbial and foreign surface (Lambris et al. 1999).

Understanding the mechanism of action of bioactive polysaccharides toward biological cascades requires a fine knowledge of the binding properties to target proteins and of the carbohydrate structure. Much effort has been taken during the past years to elucidate the structure of fucoidan, using high-field nuclear magnetic resonance (NMR) (Chevolot et al. 1999; Daniel et al. 1999; Bilan et al. 2002) and mass spectrometry (Daniel et al. 2007). The widely studied fucoidan from *Ascophyllum nodosum*, a brown alga of the fucale order, has a [→4)-α-L-Fuc*p*-(1→3)-α-L-Fuc*p*-(1→4)-α-L-Fuc*p*-(1→3)-α-L-Fuc*p*(1→] backbone with sulfate groups mainly on the C2 position of the fucosyl units (Chevolot et al. 2001; Daniel et al. 2001). Much less is known about the mechanism and the structural determinants involved in the interactions with targetted proteins. We have previously reported that *A. nodosum* fucoidan inhibits the first steps of the complement cascade through specific interactions with target proteins belonging to the classical pathway, particularly the complement protein C4 (Tissot et al. 2003; Tissot et al. 2005). However, the structural characteristics of the polysaccharide required for this anticomplement activity remained to be established.

[1]To whom correspondence should be addressed: Tel: +33-1-69-47-7641; Fax: +33-1-69-47-7655; e-mail: regis.daniel@univ-evry.fr
[2]Present address: Division of Molecular Biosciences, Imperial College, South Kensington Campus, Exhibition Road, SW7 2AZ, London, UK.

Table I. Inhibition of complement by fucoidan oligosaccharides. Complement activity was determined by the measure of the hemolysis of sensitized erythrocytes. IC_{50} is the amount (μg) of fucoidan inhibiting 50% of the complement-mediated hemolysis

Oligosaccharide	Molecular weight[a] ($g\ mol^{-1}$)	Sulfate (SO_3Na) (%)	Complement inhibition IC_{50} (μg)
Pentasaccharide	1420	45.8	>50
F1	3090	37	32
F2	3200	34	3

[a]Molecular weight determined by size-exclusion chromatography for F1 and F2. Molecular weight calculated for the synthetic pentasaccharide.

In order to identify the structural determinants of fucoidan involved in the interaction with the protein C4, low molecular weight (LMW) fractions of fucoidan from the brown algae *A. nodosum* as well as a synthetic pentasaccharide reproducing the structure repeat found in fucoidan (Hua et al. 2004) have been analyzed in the study herein by high-field solution NMR including saturation transfer difference-NMR (STD-NMR) (Mayer and Meyer 1999; Mayer and Meyer 2001) and transfer nuclear Overhauser effect spectroscopy (TRNOESY) experiments (Clore and Gronenborn 1982; Clore and Gronenborn 1983). While STD-NMR experiments allow the identification of the ligand protons in direct con-

Table II. ^1H and ^{13}C chemical shifts of the fucose residues in the LMW fucoidan fractions F1 and F2[a] and in the synthetic pentasaccharide

Residue		Fraction	H1/C1	H2/C2	H3/C3	H4/C4	H5/C5	H6/C6
A								
→4)-α-L-Fucp-(2,3-di-SO_3^-)-(1→3)-	A_p^1	*Penta*	5.45/97.8	4.69/75.4	4.82/76.7	4.30/82.3	4.66/70.7	1.43/18.5
	A_p^2	*Penta*	5.45/96.5	4.71/75.4	4.89/76.7	4.32/82.5	4.72/70.6	1.44/18.5
	A^1	*F1*	5.48/97.0	4.71/75.2	4.86/76.9	4.32/82.1	4.61/70.6	1.40/18.4
		F2	5.50/97.0	4.73/75.3	4.89/76.5	4.33/81.5	4.64/70.7	1.46/18.3
	A^2	*F1*	5.45/97.5	4.69/75.2	4.86/76.9	4.32/82.1	4.61/70.6	1.40/18.4
		F2	5.47/97.5	4.71/75.3	4.85/76.8	4.34/82.1	4.64/70.7	1.46/18.3
	A^3	*F2*	5.45/97.9	4.69/75.3	4.83/76.8	4.31/82.3	4.65/70.2	1.44/18.3
	A^4	*F2*	5.35/96.2	4.68/74.7	4.92/76.3	4.37/82.4	4.38	1.25
B								
→3)-α-L-Fucp-(2-SO_3^-)-(1→4)-	B_p	*Penta*	5.34/101.7	4.63/76.3	4.27/76.4	4.18/72.5	4.47/69.9	1.35/18.2
	B^1	*F1*	5.30/101.4	4.65/76.0	4.26/76.0	4.17/72.0	4.50/69.4	1.31/18.2
		F2	5.32/101.3	4.65/76.1	4.28/75.6	4.18/72.0	4.54/69.5	1.36/18.2
	B^2	*F1*	5.34/101.4	4.62/76.0	4.26/76.0	4.17/72.0	4.50/69.4	1.31/18.2
		F2	5.36/101.5	4.63/76.3	4.27/76.1	4.17/72.5	4.49/69.9	1.35/18.2
	B^3	*F2*	5.28/101.8	4.64/76.2	4.23/74.5	4.19/71.1	4.54/69.7	1.28/18.2
	B^4	*F2*	5.39/101.7	4.62/76.6	4.27/76.0	4.17/72.2	4.40/70.1	1.35/18.2
	B^5	*F2*	5.34/102.0	4.63/76.2	4.24/76.2	4.17/72.5	4.40/70.1	1.31/18.2
B′								
→3)-α-L-Fucp-(2,4-di-SO_3^-)-(1→4)-	B′	*F2*	5.38/101.2	4.62/76.6	4.50/76.2	4.93/84.8	4.54/nd	1.32/18.2
C								
α-L-Fucp-(2,3-di-SO_3^-)-(1→3)-	***C***	*F1*	5.43/97.5	4.61/75.3	4.78/78.1	4.27/73.7	nd	nd
		F2	5.44/97.4	4.62/75.3	4.78/77.9	4.27/73.5	4.63/69.4	1.31/18.2
C′								
α-L-Fucp-(2-SO_3^-)-(1→3)-	C′	*F2*	5.41/96.8	4.51/78.2	4.22/70.3	3.95/75.3	4.29/68.8	1.22/18.2
D								
α-L-Fucp-(2-SO_3^-)-(1→4)-	***D***	*Penta*	5.30/101.6	4.51/78.5	4.22/70.2	3.98/75.2	4.51/70.2	1.33/18.1
		F1	5.30/101.0	4.50/78.0	4.20/70.2	3.97/75.3	nd	nd
		F2	5.31/101.4	4.51/78.4	4.22/70.1	3.98/75.0	4.50 /70.2	1.32 /18.2
E								
→4)-α-L-Fucp-(2,3-di-SO_3^-)	***E***	*F1*	5.58/93.4	4.64/nd	4.73/nd	4.34/nd	nd	nd
		F2	5.60/93.5	4.65/75.8	4.74/77.0	4.35/82.7	4.39/70.0	1.44/18.3
E′								
→4)-α-L-Fucp-(2-SO_3^-)	E′	*F2*	5.54/93.3	4.47/78.7	4.09/70.5	4.05/85.7	4.38/69.9	1.42/18.3
F								
→3)-α-L-Fucp-(2-SO_3^-)	***F***	*Penta*[b]	4.59/104.2	4.38/78.8	3.94/79.1	4.09/70.6	3.84/73.4	1.34/18.2
		F1	5.52/93.4	4.57/nd	4.11/nd	4.14/nd	nd	nd
		F2	5.54/93.4	4.58/76.2	4.13/76.2	4.15/70.2	4.28/68.8	1.29/18.2
G								
→3,4)-α-L-Fucp-(2-SO_3^-)-(1→3)-	G	*F2*	5.47/95.8	4.56/78.1	4.27/76.0	4.04/84.8	4.55/70.4	1.43/18.3
G′								
→4)-α-L-Fucp-(2-SO_3^-)-(1→3)-	G′	*F2*	5.42/96.8	4.52/78.2	4.21/70.5	4.06/85.4	4.61/nd	1.41/nd

Superscripts "[1, 2], etc." are used to distinguish residues having the same substitution pattern but displaying slightly different chemical shifts (fractions F1 and F2). Subscript "p" refers to residues belonging to the pentasaccharide.

[a]Chemical shifts were measured on COSY and HSQC spectra recorded with a 600-MHz spectrometer. Values for the fraction F1 are from (Chevolot et al. 2001. Carbohydr. Res 330: 529–535).

[b]The terminal F residue at the reducing end of the synthetic pentasaccharide was in β form and substituted by an octyl chain at position C1 (^1H chemical shifts of the octyl chain are 0.91, 1.36, 1.41, 1.66, 3.72 and 3.90).

D **Ap^1** **B**
α-L-Fuc*p*-2(OSO3$^-$)-(1→4)-α-L-Fuc*p*-2,3(OSO3$^-$)$_2$-(1→3)-α-L-Fuc*p*-2(OSO3$^-$)-(1→
Ap^2 **F**
4)-α-L-Fuc*p*-2,3(OSO3$^-$)$_2$-(1→3)-α-L-Fuc*p*-2(OSO3$^-$)-OC8H17

Scheme I. Structural organization of the synthetic fucoidan pentasaccharide.

tact with the protein receptor, TRNOESY experiments give rise to distance data useful to calculate the receptor-bound ligand conformation. The combination of these two experiments has previously been fruitfully used for studying the interaction between carbohydrates and various proteins such as antibodies and enzymes (Angulo et al. 2006; Clement et al. 2006). Our goals were to identify the regions of fucoidan in close contact with the protein and determine the carbohydrate-bound structure. The structure data were confronted to the anticomplementary activities of the fucoidan fraction in order to decipher their structure–function relationship. The results underline the importance of oligosaccharide branching in the anticomplementary activity.

Results and discussion

Anticomplementary activity of LMW fucoidan

The fucoidan fractions studied in this work were of LMW, i.e. below 3500 g mol^{-1}. We first evaluated their inhibitory activity towards the human complement system in whole serum using a hemolytic assay. The anticomplementary activities were surprisingly different from one fraction to another (Table I). The synthetic pentasaccharide (M_W 1420 g mol^{-1}) reproducing the structure repeat found in fucoidan was inactive. Fraction F1 (M_W 3090 g mol^{-1}) exhibited a weak anticomplementary activity despite its high sulfate content (37%). The most active fraction was F2 (M_W 3200 g mol^{-1}). This fraction has a slightly lower sulfate content and a molecular weight comparable to the one of fraction F1. Hence, the inhibiting activity was not only dependent on molecular weight but also relied on structural determinants such as sulfate pattern and oligosaccharide backbone organization. To better understand these relationships, we investigated the structural determinants of the active fraction F2 using NMR spectroscopy and compared this refined structural data with the ones of a LMW fucoidan F1 and a synthetic pentasaccharide previously described (Chevolot et al. 1999; Chevolot et al. 2001; Hua et al. 2004).

Structure of LMW fucoidan F1 and synthetic pentasaccharide

F1 had been described as a mixture of linear oligosaccharides of approximately 8–14 residues and constituted mainly by alternating 2,3-*O*-sulfated fucose units [α-L-Fucp-2,3(OSO3)$_2$-1→3] and 2-*O*-sulfated fucose units [α-L-Fucp-2(OSO3)-1→4] named residues A and B, respectively (Chevolot et al. 2001). The same residue nomenclature is used in this study, i.e. 2,3-*O*-disulfated residues A have terminal counterpart residues C and E at the nonreducing and reducing ends, respectively, and 2-*O*-sulfated residues B have terminal counterpart residues D and F at the nonreducing and reducing ends, respectively. In this fraction and in the two others described here, each type of residue with a single substitution pattern could be found at slightly different chemical shifts. For example, two types of residue A (A^1 and A^2) showing small differences in H1 and H2 chemical shifts (Table II) were identified in Fraction 1 spectrum. The same observation was made for residue B which also exists under two forms, B^1 and B^2 (Table II). These differences may arise from different conformational equilibria at nearby glycosidic linkages.

The complete NMR attribution of the synthetic fucoidan pentasaccharide (Table II) was performed for the first time

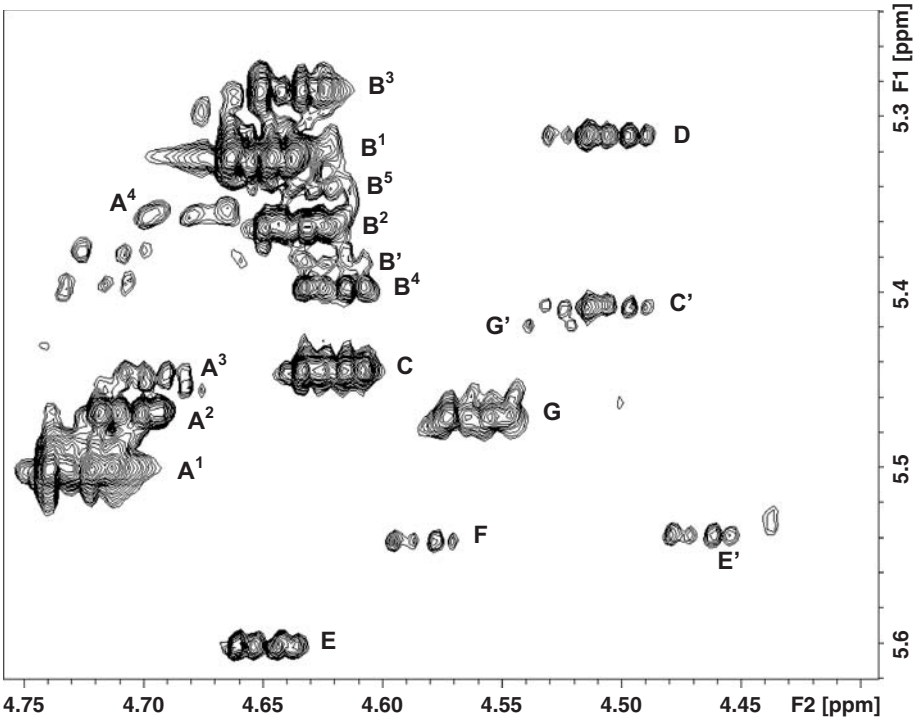

Fig. 1. Region of the COSY spectrum of the fraction F2 showing the H1/H2 cross-peaks. The corresponding residues are labeled.

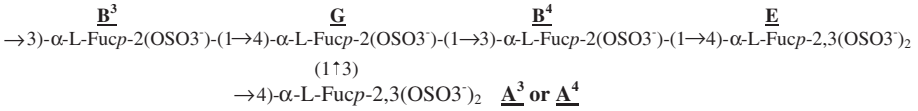

Scheme II. Structural organization of the branched fucoidan F2.

and it confirmed its linear structure composed of alternating 2,3-*O*-disulfated fucose and 2-*O*-monosulfated fucose (Scheme I) (Hua et al. 2004). Both disulfated residues in the pentasaccharide (type A residues) could be distinguished from each other through slight difference in the chemical shift of their H3 and H5, indicating subtle difference in their environment along the oligosaccharide chain (referred as residues Ap^1 and Ap^2 in Table II). It is worth noting that for linear chain the *O*-glycosidic bond of either 1→3 or 1→4 linkage has a clear influence on the chemical shift of the α anomeric proton and carbon, respectively, 5.4–5.5 ppm and 94–97 ppm for the 3-linked anomeric atoms and 5.3 ppm and 101–102 ppm for the 4-linked ones.

Structural data of LMW fucoidan F2

Although being in the same molecular weight range than fraction F1, fraction F2 exhibited a more crowded NMR profile revealing the complexity of this fraction. Assignments (Table II) were made based on previously published NMR data (Chevolot et al. 2001; Daniel et al. 2001; Mulloy et al. 2000) and by using the aforementioned values obtained from the synthetic pentasaccharide. The H1–H2 cross-peaks in correlation spectroscopy (COSY) spectrum (Figure 1) belonging to 18 different spin systems have been identified, some of them being weakly represented. They can be distributed as follows in four groups according to their sulfation pattern and the nature of their glycosidic linkages (see detailed assignments in Supplementary data).

Residues of type A [*→4)-α-L-Fucp-2,3di(OSO_3^-)-(1→3*] were composed of four kinds of residues (A^1–A^4) corresponding to slight differences on the H1–H2 cross-peak positions. We assumed that for all residues A protons up to H4 were in very similar environments given their almost identical spin systems (Table II). Integration of all residues A anomeric protons indicated that they accounted for around 40% of all F2 anomeric protons. This proportion was confirmed by the integration of the sharper H4 signal.

Five kinds of residues of type B [*→3)-α-L-Fucp-2(OSO_3^-)-(1→4*] (B^1–B^5) were distinguished. Although identically substituted, i.e. 2-*O*-sulfated, these residues presented slightly different anomeric proton H1 chemical shifts, suggesting that each anomeric position was linked to nonequivalent residues or at least, involved in different local conformations. An additional type of residue B (B′) was detected that was attributed to a 2,4 disulfated fucose. Integration of all residues B H1 signals showed that they accounted for about 50% of all anomeric protons.

2,3-*O*-disulfated and 2-*O*-sulfated fucose named residues E and F, respectively, were identified as terminal residues at the reducing end as in the fraction F1. In the same way, 2,3-*O*-disulfated and 2-*O*-sulfated residues named, respectively, C and D were detected at the nonreducing ends.

Finally, a branching residue named G was distinguished on COSY spectrum (Figure 1) as being a 2-*O*-sulfated fucose engaged in two *O*-glycosidic bonds at positions 3 and 4 in addition to its 1→3 linkage. Consequently, G was defined as a branching residue [3,4-di-*O*-disusbtituted-α-L-Fucp(2-SO_3^-) 1→3]. This was confirmed by the heteronuclear multiple bond correlation (HMBC) spectrum (see below).

HMBC connectivities: H1/C3 and H1/C4 connectivities showed that residues A were linked to the position 3 of residues B and that residues B were linked to the position 4 of residues A, respectively. Concerning the branching residue G, a cross-peak observed between its C4 and the H1 of B^3 indicated that the 4-position of G was linked to B^3. Concerning the second substitution of G, the correlation peaks C1/H3 at 97.9/4.27 and 96.2/4.27 ppm argued for a linkage between a residue A (A^3 or A^4) with the C3 of residue G. Moreover, connectivity observed between C1 of G and H3 of B^4 (95.8/4.27 ppm) showed that G was linked to position 3 of B^4. Finally, the structural organization around the branching residue G found in the fucoidan oligosaccharides of the fraction F2 is represented in Scheme II.

Overall, NMR data indicated that fraction F2 was constituted of oligosaccharides characterized by the same backbone as fraction F1 with alternate 2,3-*O*-sulfated fucose unit [α-L-Fucp-2,3($OSO3)_2$-1→3] (residue A) and 2-*O*-sulfated fucose unit [α-L-Fucp-2(OSO3)-1→4] (residue B), i.e. showing alternate (1→3)- and (1→4)-linkage in agreement with the polysaccharide backbone ascribed to fucoidan from fucale algae (Kusaykin et al. 2008). However, unlike F1, F2 exhibited branching chains. In order to determine whether the branching played a role in the inhibitory effect of the fraction F2 towards the human complement system (Table I), the interaction of F2 with the protein C4 was studied by STD-NMR analysis.

Characterization of fucoidan interaction with the complement protein C4 by STD-NMR

We have previously reported a dissociation constant of 5.0×10^{-6} M of fucoidan interacting with the protein C4 (Tissot et al. 2003). This value is compatible with STD-NMR experiments, which required K_D values between 10^{-3} and 10^{-8} M (Mayer and Meyer 1999; Mayer and Meyer 2001). Thus, STD-NMR methods were used to pinpoint in 1D spectra, the STD enhanced proton signals of the fraction F2 in close contact with the protein C4, taking into account that the largest effect is observed for the closest proton. The 1D STD spectrum of the fraction F2 in interaction with the protein C4 showed a significant resonance overlap between 4 and 4.7 ppm, hampering the specific assignment of the STD signals in this region. However, clear STD signals could be analyzed for anomeric and methyl protons (Figure 2 and Table III), which were assigned with conventional 2D NMR spectra performed prior to the STD experiments (Table 1S in Supplementary data). Regarding the anomeric region, the largest STD enhancement was observed for the H1 of the reducing end residue E (5.59 ppm) (Figure 2C). This latter was therefore used as reference (100%) for the calibration of the STD effects. Interestingly, significant STD enhancements were also observed for the H1 (65%) of the

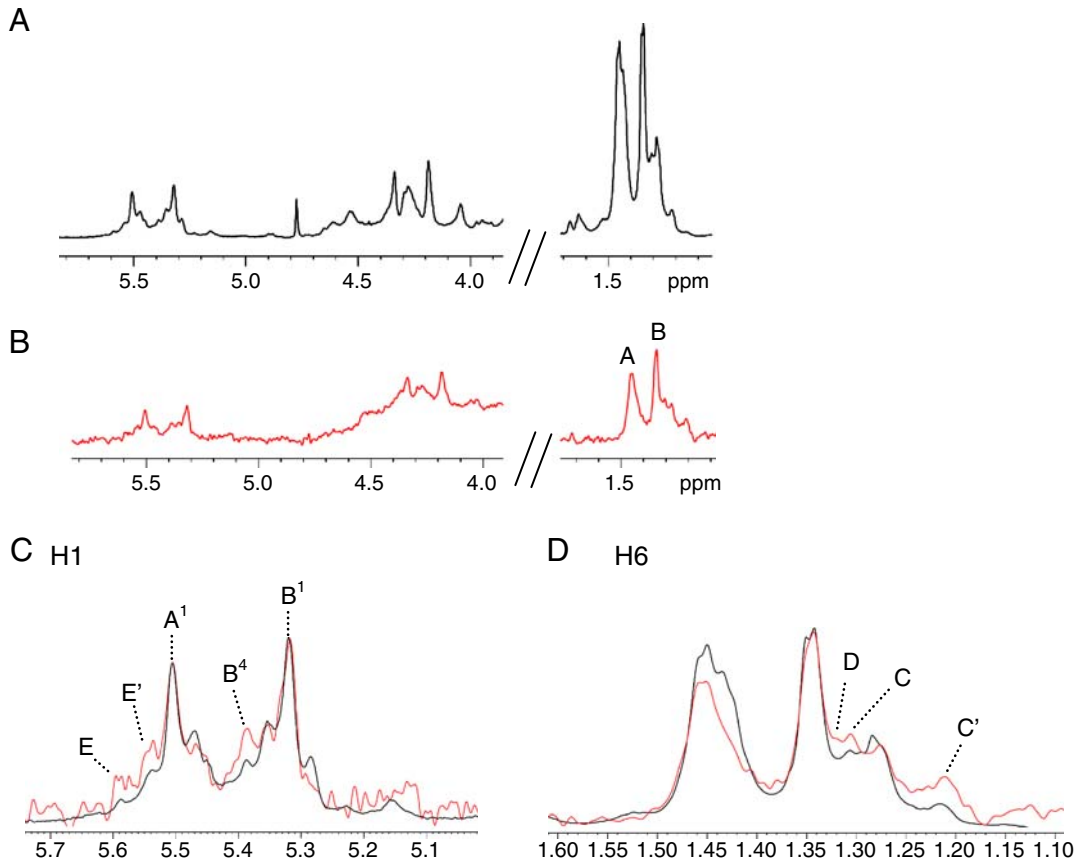

Fig. 2. (**A**) 1D ^{1}H NMR spectrum of the fraction F2 in D_2O. (**B**) 1D STD-NMR spectrum of the fraction F2 in the presence of the protein C4. The selective saturation of protein protons has been applied at 7 ppm. The methyl groups of the type A and B residues are labeled. Superposition of (**C**) anomeric and (**D**) methyl regions the 1D spectrum of the fraction F2 alone (in black) and the 1D STD-NMR spectrum of the fraction F2 in the presence of the protein C4 (in gray). The intensity of the 1D STD-NMR spectrum is normalized against the more intense signals of the 1D spectrum. The labeled protons are, among the unambiguously resolved protons, those being the most affected by the selective saturation of protein.

residue B^4 linked to the C4 position of the residue E (Scheme II), and for the H1 (62%) of the residue E′ that corresponds to a residue E having lost its 3-*O*-sulfate group. In addition, the H1 of residue A^1 gave an STD effect (43%) slightly higher than the one of residue B^1 (41%) (Figure 2C). Concerning the methyl region, the methyl protons belonging to type B residues (1.34–1.35 ppm) were in average more enhanced (around 25%) than those of the type A residues (1.43–1.46 ppm) (around 20%) (Figure 2B), the strongest enhancements being observed for the nonreducing residues (C, C′ and D) (Figure 2D).

For comparison, the same study was also undergone with the synthetic pentasaccharide which contrary to the fraction F2 does not show anticomplementary activity. STD-NMR data obtained for the synthetic pentasaccharide showed that all residues of the oligosaccharide interacted with the protein C4 (Figure 3). The most enhanced signal was observed for the methyl group of the octyl chain of the pentasaccharide and was used as reference (100%) (Figure 3B). Among the different residues of the pentasaccharide, the reducing end residue F showed the strongest enhancements (Figure 3C). Additionally, the methyl protons of residues Bp, D and F exhibited about twice stronger enhancement than to those of residues Ap (Figure 3B). Even if the low temperature (279 K instead of 303 K used for the fraction F2, see Materials and methods section) used here might favor biomolecular interaction (Haselhorst et al. 2004; Haselhorst et al. 2007), this STD experiment showed unambiguously that the pentasaccharide interacts with the protein C4 despite its lack of anticomplementary activity.

Together, STD-NMR data showed that both fraction F2 and synthetic pentasaccharide interact with the protein C4, the re-

Table III. STD enhancement[a] (%) for the fucoidan fraction F2 and the synthetic pentasaccharide in interaction with the protein C4

Fraction F2		Synthetic pentasaccharide	
H1 A^1	43	H1 F	59
H1 B^1	41	H2 F	88
H1 B^4	65	H3 F	61
H1 E	100	H4 F	61
H1 E′	62	H5 F	67
H6 C	34	H6 F	51
H6 C′	68	H6 $A_p^{1,2}$	23
H6 D	36	H6 B_p	54
		H6 D	51
		CH2α o[b]	73
		CH2β o	67
		CH3 o	100

[a]STD enhancement was the ratio I_{STD}/I_0 of the STD signal intensity (I_{STD}) to the intensity of the corresponding signal in 1D reference spectra (I_0) and then normalized with respect to the largest value.
[b]Protons of the octyl chain at position C1 of the residue F.

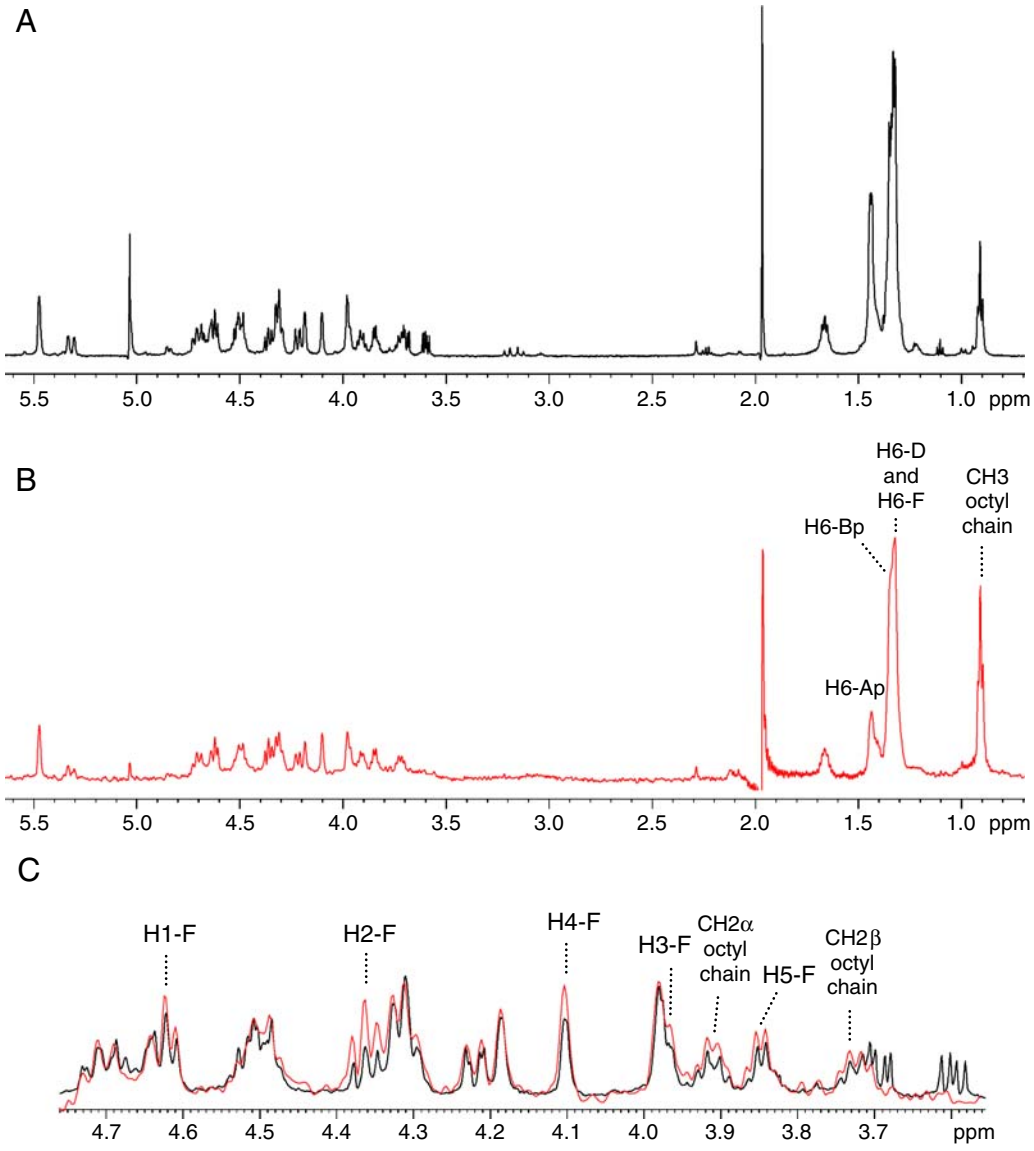

Fig. 3. (**A**) 1D ^{1}H NMR spectrum of the synthetic pentasaccharide in D_2O. (**B**) 1D STD-NMR spectrum of the pentasaccharide in the presence of the protein C4. The selective saturation of protein protons has been applied at 7 ppm. The methyl groups are labeled. (**C**) Superposition of a region of the 1D spectrum of the pentasaccharide alone (in black) and the 1D STD-NMR spectrum of the pentasaccharide in the presence of the protein C4 (in gray). Protons, the most affected by the selective saturation of protein, are labeled.

ducing end residues being in close proximity to the protein. Moreover, the methyl groups of type B residues appear to be in closer interaction with the protein than those of type A. The nonreducing residues seem to be also important for the C4 recognition. Thus, the protein C4 seems to have preferential binding sites on the fucoidan oligosaccharides. To delineate the spatial arrangement of these binding sites, we attempted to determine the C4-bound conformations of the oligosaccharides using TRNOESY experiments.

Free and C4-bound conformations of the synthetic fucoidan pentasaccharide

TRNOESY experiments were performed in the same conditions than the ones used for STD-NMR. The fraction F2 encompassing a large number of residues with close chemical shifts, the 2D TRNOESY spectrum of F2 in interaction with the protein C4 could not be accurately analyzed. We thus focused our analysis on the synthetic fucoidan pentasaccharide, thereafter named DABAFo.

Before studying the C4-bound conformation, we performed the structural analysis of the free structure of DABAFo at two temperatures 279 and 303 K. 2D nuclear Overhauser enhancement spectroscopy (NOESY) spectrum recorded at 303 K showed a smaller number of peaks characterized by a weaker intensity than those observed at 279 K (Table IV, Figures 4 and 1S). This observation is consistent with a higher flexibility of DABAFo upon temperature elevation.

The free DABAFo structure, determined by using distance data (Table IV) derived from 2D NOESY spectra, exhibited curved conformations at 303 and 279 K (Figure 5A and B). According to the glycosidic dihedral angles (Table V), the B–

Table IV. Interglycosidic NOEs and TRNOEs observed for the synthetic pentasaccharide DABAFo in free and C4-bound forms, respectively

	Intensity[a]		
	Free DABAFo		C4-bound DABAFo
Protons pairs	279 K	303 K	279 K
H1 D/H4 Ap^1	m	m	s
H1 D/H3 Ap^1	–	–	w
H1 D/H6 Ap^1	w	w	w
H5 D/H2 Ap^1	–	m	m
H3 D/H2 Ap^1	–	–	w
H6D/H1 Ap1	–	–	w
H1 Ap^1/H3 B	s	s	s
H1 Ap^1/H4 B	s	s	s
H1 Ap^1/H5 B	–	w	m
H2 Ap^1/H4 B	w	w	m
H1 B/H4 Ap^2	s	s	s
H1 B/H5 Ap^2	–	–	w
H1 B/H3 Ap^2	–	–	w
H1 B/H6 Ap^2	w	w	w
H5 B/H2 Ap^2	m	m	m
H3 B/H2 Ap^2	m	–	–
H3 B/H6 Ap^2	w	m	m
H6 B/H2 Ap^2	–	–	w
H6 B/H1 Ap^2	–	–	w
H1 Ap^2/H3 F	s	s	s
H1 Ap^2/H4 F	s	s	s
H1 Ap^2/H5 F	–	w	m
H2 Ap^2/H4 F	–	w	m
H5 Ap^2/H3 F	w	w	m

[a] s, strong; m, medium; w, weak.

A linkages (D–Ap^1 and B–Ap^2) at 303 K were more flexible (particularly the Ψ angles) than the A–B linkages (Ap^1–B and Ap^2–F). Nevertheless, the flexibility of the B–A linkages decreased with temperature as showed by Φ and Ψ values at 279 K. As a consequence, the methyl groups of residues B lined up on a same side along the oligosaccharide backbone in the average free structure at 279 K (Figure 5B).

2D TRNOESY experiment was performed at 279 K for the structural analysis of C4-bound DABAFo (Figures 4C and 1Sc). Compared to the NOESY, the TRNOESY showed additional peaks corresponding to TRNOEs induced upon C4 binding. Moreover, some peaks were reinforced in the presence of C4, for example H1 Ap^2/H5 F and H1 Ap^1/H5B, revealing conformation changes upon complex formation (Figure 4C). The C4-bound calculated structures derived from interglycosidic TRNOEs (Table IV) were characterized by well-defined glycosidic dihedral angles (Table V) coherent with a rather rigidity of the pentasaccharide in the complex. Unlike curved conformations observed for the average free structures, the average bound structure of DABAFo showed a regular linear conformation with sulfate and methyl groups of residues A and B pointing in opposite directions (Figure 5C). In this linear conformational arrangement, three sulfate groups are carried by the side of residues A methyl groups whereas four sulfate groups are on the side of residues B methyl groups. Therefore, this latter side is the most negatively charged (Figure 5C). As methyl groups of residues B are in closer protein contact than methyl groups of residues A according to STD-NMR data, we assumed that binding to protein C4 involves the most negatively charged side of the pentasaccharide.

Interestingly, the conformation of the bound state of the pentasaccharide appears close to the free structure observed at 279 K. As at this low temperature, we noted that this free state of the pentasaccharide was also more constrained, we suggest that this more rigid conformational behavior of the molecule may be a key point in the fucoidan-C4 recognition.

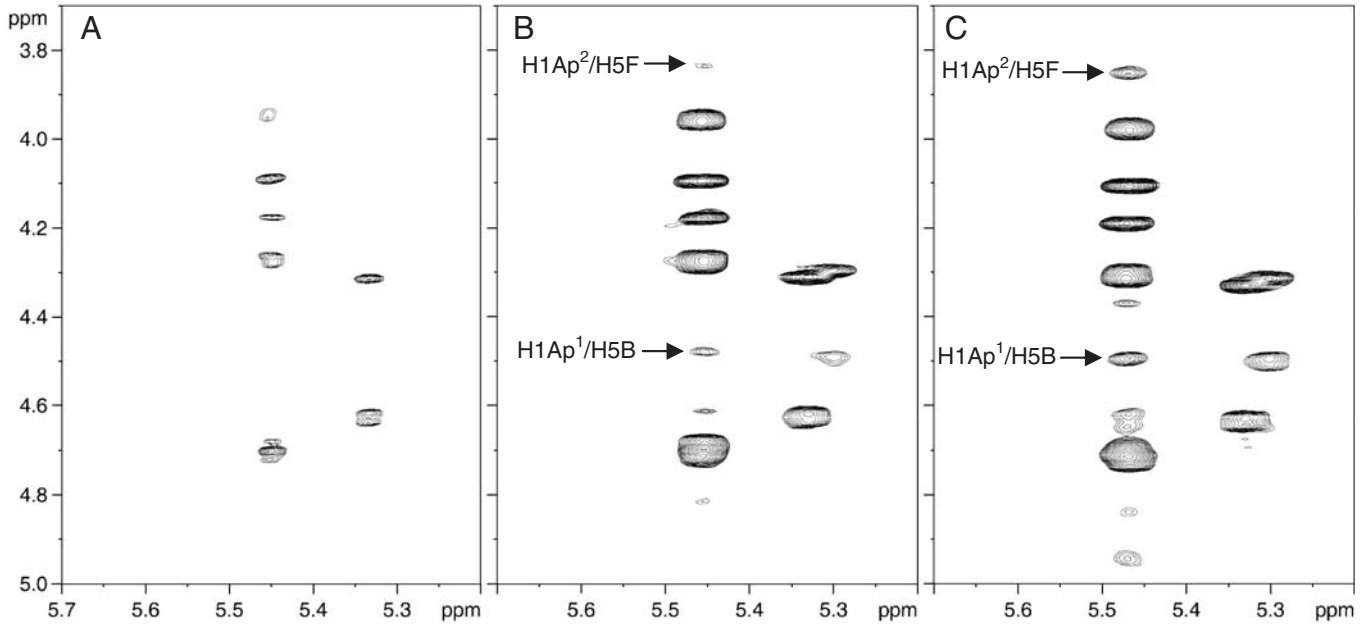

Fig. 4. Anomeric region of the 2D NOESY spectrum of the pentasaccharide DABAFo at (**A**) 303 K (4 mM) and (**B**) 279 K (240 μM) in D_2O. (**C**) Anomeric region of the TRNOESY spectrum of DABAFo recorded at 279 K in the presence of the protein C4 with a 100:1 pentasaccharide:protein ratio (240 μM pentasaccharide and 2.4 μM protein) in 135 mM NaCl, 15 mM sodium phosphate buffer pH 7.2. Spectra were recorded at 600 MHz with a mixing time of 200 ms. Two interglycosidic NOEs showing changes in pentasaccharide conformation behavior are labeled upon (B) a decrease of temperature and (C) upon interaction with the protein C4.

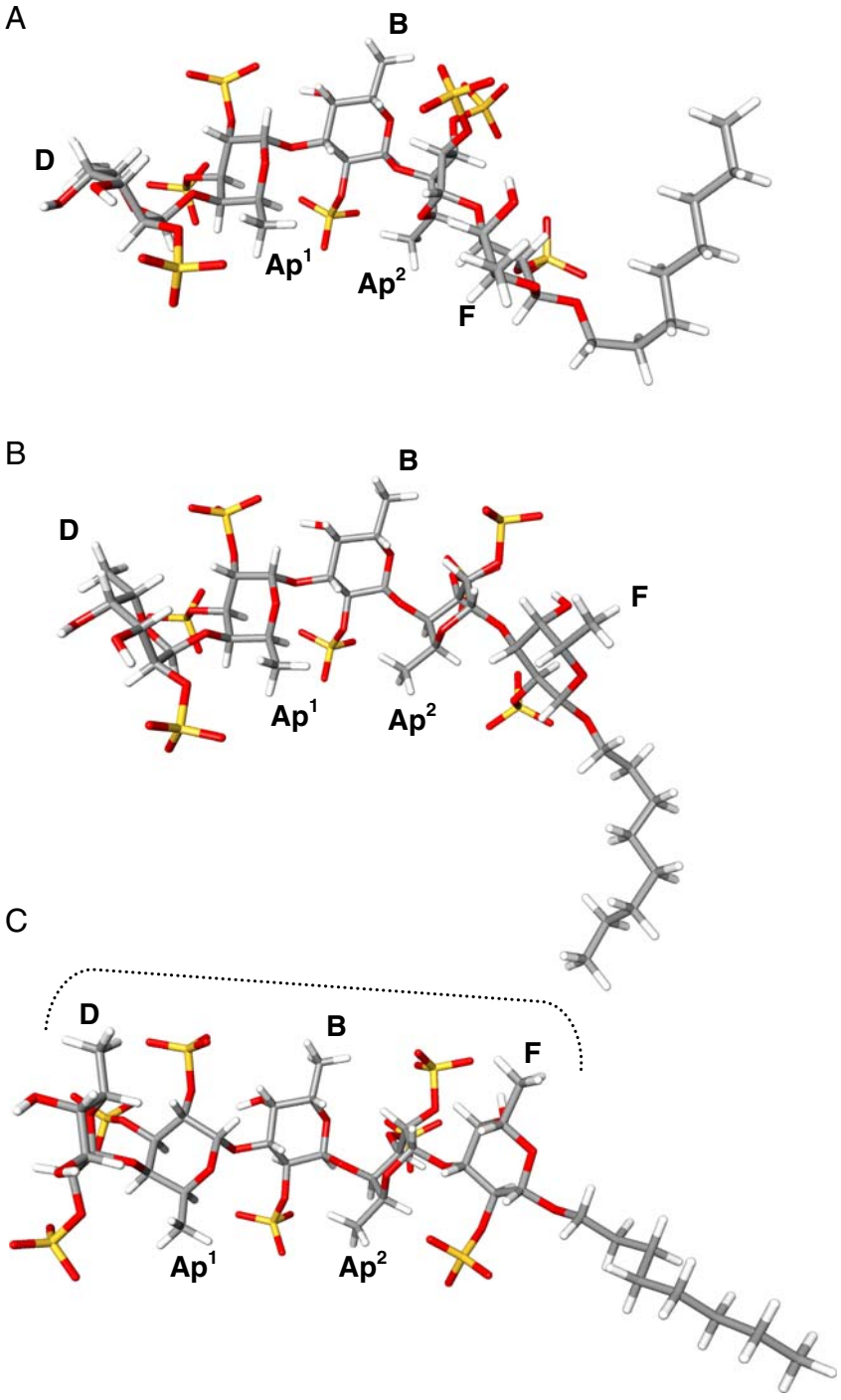

Fig. 5. Average structures of the pentasaccharide DABAFo obtained in solution from NMR data at 303 K (**A**) and 279 K (**B**) and in presence of C4 (**C**). A dashed line brackets the pentasaccharide side that is in closer contact with the protein C4 according to STD-NMR data. The name of each residue is labeled at the level of its methyl group. The molecules are visualized with Sirius software (http://sirius.sdsc.edu/).

Influence of side chains on the conformation of the fucoidan oligosaccharide backbone

Unlike the inactive pentasaccharide DABAFo, the anticomplementary fraction F2 exhibited a branching point. In order to determine the influence of side chain(s) on the conformation of the oligosaccharide backbone and its/their contribution(s) to the anticomplementary activity of F2, we have carried out the molecular modeling of a branched pentasaccharide (D(A) GBAFo) and compared it to the linear structure DABAFo.

As a first step, the conformational behaviors of two disaccharides representative of the two linkages (A–B and B–A) founded in the pentasaccharide DABAFo were determined by building Φ/Ψ/Energy maps (Figure 6). As observed above by NMR, the B–A linkage appeared more flexible (particularly

Table V. The glycosidic dihedral angles (Φ, Ψ) of the 10 lowest energy conformations of the pentasaccharide DABAFo in free and C4-bound forms and of the branched structure D(A)GBAFo

Glycosidic dihedral angles Φ/Ψ (°)		NMR data			Molecular modeling data	
		Free DABAFo		C4-bound DABAFo		
		303 K	279 K	279 K	DABAFo	D(A)GBAFo
D-A_p^1	Min	−80/−98	−80/−100	−103/−160	−80/−101	−100/−155
	Max	−105/−160	−105/−160	−107/−162	−105/−159	−106/−160
	Average	**−93/−133**	**−95/−143**	**−106/−161**	**−96/−143**	**−104/−158**
	SD	*11/29*	*9/22*	*1/1*	*10/23*	*2/2*
A_p^1-B	Min	−69/−74	−71/−72	−102/−73	−71/−71	−71/−75
	Max	−81/−83	−78/−81	−107/−77	−85/−84	−78/−81
	Average	**−73/−79**	**−73/−76**	**−105/−75**	**−75/−79**	**−74/−78**
	SD	*4/4*	*2/3*	*1/1*	*4/5*	*3/2*
B-A_p^2	Min	−78/−96	−96/−150	−101/−161	−80/−108	−92/−142
	Max	−99/−143	−111/−161	−106/−163	−106/−157	−110/−157
	Average	**−89/−133**	**−103/−156**	**−103/−161**	**−98/−148**	**−102/−152**
	SD	*5/18*	*5/4*	*2/1*	*8/15*	*2/1*
A_p^2-F	Min	−73/−69	−73/−70	−95/−73	−72/−71	−71/−72
	Max	−78/−81	−80/−81	−98/−75	−77/−77	−81/−83
	Average	**−76/−74**	**−75/−75**	**−96/−74**	**−74/−74**	**−75/−77**
	SD	*2/4*	*3/4*	*1/1*	*2/2*	*4/4*

SD, standard deviation.

the Ψ angle) than the A–B linkage. The Φ and Ψ angle values corresponding to the lowest energy region of each linkage were used as constraints to model the pentasaccharide DABAFo and the branched structure D(A)GBAFo. The modeling of DABAFo based on the Φ/Ψ/Energy map led to calculated structures very close to the free structures determined by NMR (Table V). With regard to the calculated structures of the branched oligosaccharide D(A)GBAFo, the introduction of a side chain led to a decrease of flexibility of both B–A-type linkages D–Ap^1 and B–Ap^2 (Table V) and resulted in a conformation close to the one recognized by the protein C4 (Figure 2S in Supplementary data). Hence, it can be assumed that ramification may increase the affinity of branched fucoidan for the protein C4 and led to a stronger anticomplementary activity as observed for the fraction F2.

Conclusion

Fucoidans are considered as branched polysaccharides; however, their ramifications are rarely studied. Indeed the structural heterogeneity and the random sulfation of the polysaccharide chain make the characterization and localization of the branching points difficult. The fucoidan fraction F2 studied here exhibited a ramified structure, whose branching residue G was completely characterized. Residue G was fully substituted with a sulfate group at position 2 and glycosidic bonds at positions 1, 3 and 4. The ramifications of this fucoidan fraction derived from the fucale algae *A. nodosum* appeared to be short side chains of fucosyl residues as reported for fucoidan derived from other algae species (Bilan et al. 2006; Kusaykin et al. 2008). STD-NMR experiment allowed us to identify the reducing end residues and the methyl group of type B residues as being in close contact with the protein C4, likely to being responsible for an effective interaction with the complement protein. Moreover, as the nonreducing end residues could be also involved in C4 recognition, the presence of ramification could offer additional binding sites, leading to a higher activity of the ramified oligosaccharides compared to linear structures. Besides, biologically important carbohydrate–protein interactions such as in heparin/heparan sulfate-growth factor complexes appear to be driven not only by the charge distribution but also by the conformational flexibility (Mulloy 2005; Skidmore et al. 2008). It has been shown recently that the induction of the acrosome reaction by sulfated galactans depended on the flexibility of the glycosidic linkages and the anomeric configuration, which led to a proper spatial arrangement for interaction with specific receptors (Castro et al. 2009). TRNOESY experiment and molecular modeling of fucoidan oligosaccharides indicated that the presence of side chains reduces the flexibility of the backbone, which adopts a conformation close to the one recognized by the protein C4. As a consequence, the oligosaccharide epitopes in close contact with the protein appeared to be placed in the appropriate 3D orientation to allow effective interactions. Together, the results suggest that branching of fucoidan oligosaccharides plays a major role in their anticomplementary activity at the conformational level.

Materials and methods

LMW fractions of fucoidan

Fucoidan fractions used in this study were issued from crude fucoidan extracted from the brown algae *A. nodosum* as previously published (Mabeau et al. 1990; Colliec et al. 2004). LMW fraction F1 (M_W 3090 g mol^{-1}, sulfate content 37%) was prepared by acid hydrolysis and centrifugal partition chromatography as previously reported. LMW fraction F2 (M_W 3200 g mol^{-1}, sulfate content 34%) was prepared by radical hydrolysis and anion exchange chromatography as previously reported (Nardella et al. 1996). The molecular weights were determined by high-performance size-exclusion chromatography using the 1st International Reference Preparation Low Molecular Weight Heparin as calibrant (Mulloy et al. 1997).

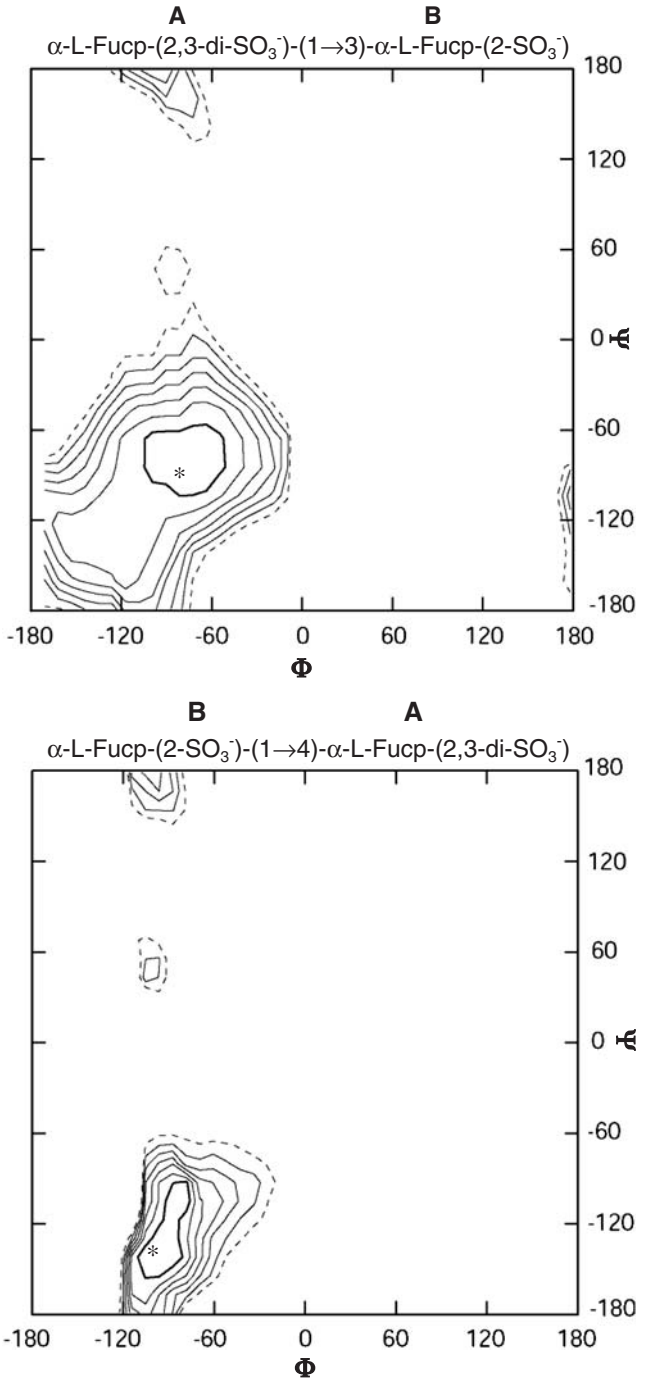

Fig. 6. Φ/Ψ Energy maps of disaccharides A–B and B–A. Iso-energy contour lines are graduated in 1 kcal/mol increments above the global minimum within a 7 kcal/mol window. The global minimum of each disaccharide is indicated with an asterisk (*). The contour lines of the lowest and highest energy region are represented in bold and dashed lines, respectively.

The synthetic fucoidan pentasaccharide (M_W 1420 g mol^{-1}) was synthesized as previously reported. Other chemicals and reagents were obtained from current commercial sources at the highest level of purity available. All buffers and sample solutions were prepared with ultrapure quality water (milliQ system, Millipore, Milford, MA).

Hemolytic assay of the anticomplementary activity in whole serum

The anticomplementary activity of the fucoidan fractions and of the synthetic pentasaccharide was assessed as described elsewhere. Briefly, the determination of IC_{50} was performed as follows: 350 µL of normal human serum (1/100 in veronal-buffered saline [VBS^2]) was incubated with 450 µL of VBS^2 containing 0–50 µg of fucoidan and 200 µL of antibody-sensitized sheep erythrocytes at 10^8 cells/mL, for 45 min at 37°C. After dilution in cold 0.15 M NaCl solution (2 mL) and centrifugation, the residual CH_{50} units of the supernatants were determined by measurement of the optical density at 414 nm and IC_{50} was then determined.

NMR analysis

All NMR experiments were performed on a Bruker Avance 600-MHz NMR spectrometer equipped with a cryoprobe, and data were processed using XWINNMR (Bruker, Rheinstetten, Germany) software. Sodium [3-trimethylsilyl 2,2′,3,3′-2H4] propionate (TSP-d4) was used as an internal reference for proton chemical shifts.

The synthetic pentasaccharide and the fraction F2 were exchanged twice with 99.8% D_2O (Saint Quentin Fallavier, France) with intermediate lyophilization and dissolved at 4 mM in 500 µL 100% D_2O. 1D proton spectra were acquired with 64 scans and 16 K data points. For ^1H and ^{13}C assignments, 2D double quantum filtered COSY, total correlation spectroscopy (TOCSY), NOESY, rotating-frame Overhauser enhancement spectroscopy (ROESY), heteronuclear single quantum coherence (HSQC) and HMBC spectra were recorded. The TOCSY experiments were acquired using the MLEV17 sequence with a mixing time of 80 ms. In the 2D NOESY and ROESY experiments, the mixing period was 200 and 300 ms, respectively. All 2D experiments were carried out with 2048 data points × 512 increments × 64 scans and a spectral width of 3000 Hz in both dimensions. The data were zero-filled to give 4096 × 1024 data matrix prior to Fourier transformation. All NMR analyses of the oligosaccharide:C4 complexes including STD-NMR and TRNOESY were carried out with 2.4 µM protein C4 prepared in 135 mM NaCl, 15 mM sodium phosphate buffer pH 7.2 containing 240 µM oligosaccharide, i.e. a 100:1 ligand:protein ratio. Concerning the pentasaccharide, experiments have been performed at low temperature (279 K) in order to shift the large water peak away from pentasaccharide resonances. 1D STD-NMR experiments were recorded with 4096 scans. The protein resonances were saturated at 7 ppm (40 ppm for reference spectra) with a cascade of 40 selective Gaussian-shaped pulses of 50-ms duration, with a 1-ms delay between each pulse, resulting in a total saturation time of 2.04 s. The irradiation value at 7 ppm was far enough from the closest oligosaccharide resonance (at 5.3 ppm for anomeric proton) to avoid direct irradiation of the ligand (Meyer and Peters 2003) as verified by recording a control STD spectrum without protein (data not shown). Subtraction of saturated spectra from reference spectra was performed by phase cycling. STD enhancements were calculated by dividing the STD signal intensities (I_{STD}) by the intensities of the corresponding signals in 1D reference spectra (I_0) and then the ratios of the intensities I_{STD}/I_0 were normalized in relation to the largest value (Meyer and Peters 2003; Haselhorst et al. 2007).

Structure calculations

Distance constraints for structure calculations of the pentasaccharide DABAFo free or in interaction with C4 were derived from 200-ms mixing time NOESY or TRNOESY spectra. The cross-peak volume was measured with NMRView (Johnson and Blevins 1994) and converted to distances using the relationship $I_{ij} / I_{ref} = (r_{ref} / r_{ij})^6$ (Baleja et al. 1990) with the distance between H4 F and H5 F (2.60 Å) as a reference. Then, the interglycosidic NOEs observed for the pentasaccharide DABAFo free or in interaction with C4 were classified according to their intensities as strong, medium and weak and translated to distance constraints of 1.8–2.8 Å, 1.8–3.5 Å and 1.8–5 Å, respectively, for molecular modeling. The structures of the pentasaccharide were calculated with TINKER 3.4, http://dasher.wustl.edu/tinker/ (Hodsdon et al. 1996) using the MM3 force field (Allinger et al. 1989; Lii and Allinger 1989a; Lii and Allinger 1989b). MM3 parameters for the sulfate groups were taken from Lamba et al. (1994). Forty initial models were generated by distance geometry (DISTGEOM) and energy-minimized with the program MINIMIZE. The 10 lowest energy structures with a maximum distance violation of no more 0.1 Å were analyzed.

Conformational behavior of the pentasaccharide was analyzed using Φ/Ψ energy maps built for the two types of disaccharides, A–B and B–A, comprising the pentasaccharide as follows. The calculations were performed on minimized disaccharides using the INSIGHT II-DISCOVER module (Accelrys, Inc., San Diego, CA). The Φ and Ψ torsion angles (defined according to the International Union of the Pure and Applied Chemistry recommendations (ref) as $\Phi = O_5–C_1–O_1–C'x$ and $\Psi = C_1–O_1–C'x–C'_{x+1}$) were driven by steps of 10° over the whole angular range. At each step, the disaccharide was energy-minimized. The Φ/Ψ energy maps were generated with the program GNUPlot-4 (www.*gnuplot*.info). Iso-energy contours were plotted at intervals of 1 kcal/mol above the global minimum within a 7 kcal/mol window.

In order to determine the influence of a side chain residue A on the conformation of an oligosaccharide backbone, made of alternate residues A and B, structure calculations were performed for the branched (D(A)GBAFo) or the linear (DABAFo) pentasaccharide with TINKER as described above. For each glycosidic linkage, the values of dihedral angles delimiting the lowest energy region of the Φ/Ψ energy maps were used as angle constraints. The disaccharide and pentasaccharide structures were built using the SWEET II program (Bohne et al. 1999).

Supplementary data

Supplementary data for this article is available online at http://glycob.oxfordjournals.org/.

Conflict of interest statement

None declared.

Abbreviations

COSY, correlation spectroscopy; HMBC, heteronuclear multiple bond correlation; HSQC, heteronuclear single quantum coherence; NMR, nuclear magnetic resonance; NOESY, nuclear Overhauser enhancement spectroscopy; ROESY, rotating frame Overhauser enhancement spectroscopy; STD, saturation transfer difference; TOCSY, total correlation spectroscopy; TRNOESY, transferred nuclear Overhauser effect spectroscopy; VBS^2, isotonic Veronal-buffered saline.

References

Allinger NL, Yuh YH, Lii JH. 1989. Molecular mechanics. The MM3 force field for hydrocarbons. 1. *J Am Chem Soc.* 111:8551–8566.

Angulo J, Rademacher C, Biet T, Benie AJ, Blume A, Peters H, Palcic M, Parra F, Peters T. 2006. NMR analysis of carbohydrate-protein interactions. *Methods Enzymol.* 416:12–30.

Baleja J, Moult J, Sykes BD. 1990. Distance measurement and structure refinement with NOE data. *J Magn Reson.* 87:375–384.

Bergamaschini L, Donarini C, Gobbo G, Parnetti L, Gallai V. 2001. Activation of complement and contact system in Alzheimer's disease. *Mech Ageing Dev.* 122:1971–1983.

Bilan MI, Grachev AA, Shashkov AS, Nifantiev NE, Usov AI. 2006. Structure of a fucoidan from the brown seaweed Fucus serratus L. *Carbohydr Res.* 341:238–245.

Bilan MI, Grachev AA, Ustuzhanina NE, Shashkov AS, Nifantiev NE, Usov AI. 2002. Structure of a fucoidan from the brown seaweed *Fucus evanescens* C.Ag. *Carbohydr Res.* 337:719–730.

Bohne A, Lang E, von der Lieth CW. 1999. SWEET - WWW-based rapid 3D construction of oligo- and polysaccharides. *Bioinformatics.* 15:767–768.

Boisson-Vidal C, Zemani F, Caligiuri G, Galy-Fauroux I, Colliec-Jouault S, Helley D, Fischer AM. 2007. Neoangiogenesis induced by progenitor endothelial cells: Effect of fucoidan from marine algae. *Cardiovasc Hematol Agents Med Chem.* 5:67–77.

Castro MO, Pomin VH, Santos LL, Vilela-Silva AC, Hirohashi N, Pol-Fachin L, Verli H, Mourao PA. 2009. A unique 2-sulfated {beta}-galactan from the egg jelly of the sea urchin Glyptocidaris crenularis: Conformation flexibility versus induction of the sperm acrosome reaction. *J Biol Chem.* 284:18790–18800.

Chevolot L, Foucault A, Chaubet F, Kervarec N, Sinquin C, Fisher AM, Boisson-Vidal C. 1999. Further data on the structure of brown seaweed fucans: Relationships with anticoagulant activity. *Carbohydr Res.* 319:154–165.

Chevolot L, Mulloy B, Ratiskol J, Foucault A, Colliec-Jouault S. 2001. A disaccharide repeat unit is the major structure in fucoidans from two species of brown algae. *Carbohydr Res.* 330:529–535.

Clement MJ, Fortune A, Phalipon A, Marcel-Peyre V, Simenel C, Imberty A, Delepierre M, Mulard LA. 2006. Toward a better understanding of the basis of the molecular mimicry of polysaccharide antigens by peptides: The example of Shigella flexneri 5a. *J Biol Chem.* 281:2317–2332.

Clore GM, Gronenborn AM. 1982. Theory and applications of the transferred nuclear Overhauser effect to the study of the conformations of small ligands bound to proteins. *J Magn Reson.* 48:402–417.

Clore GM, Gronenborn AM. 1983. Theory of the time dependent transferred nuclear Overhauser effect: Application to the structural analysis of ligand-protein complexes in solution. *J Magn Reson.* 53:423–442.

Colliec S, Boisson-Vidal C, Jozefonvicz J. 2004. A low molecular weight fucoidan fraction from the brown seaweed *Pelvetia canaliculata*. *Phytochemistry.* 35:697–700.

Daniel R, Berteau O, Chevolot L, Varenne A, Gareil P, Goasdoue N. 2001. Regioselective desulfation of sulfated L-fucopyranoside by a new sulfoesterase from the marine mollusk Pecten maximus: Application to the structural study of algal fucoidan (*Ascophyllum nodosum*). *Eur J Biochem.* 268:5617–5626.

Daniel R, Berteau O, Jozefonvicz J, Goasdoue N. 1999. Degradation of algal (*Ascophyllum nodosum*) fucoidan by an enzymatic activity contained in digestive glands of the marine mollusc *Pecten maximus*. *Carbohydr Res.* 322:291–297.

Daniel R, Chevolot L, Carrascal M, Tissot B, Mourao PA, Abian J. 2007. Electrospray ionization mass spectrometry of oligosaccharides derived from fucoidan of *Ascophyllum nodosum*. *Carbohydr Res.* 342:826–834.

Haselhorst T, Blanchard H, Frank M, Kraschnefski MJ, Kiefel MJ, Szyczew AJ, Dyason JC, Fleming F, Holloway G, Coulson BS, et al. 2007. STD NMR spectroscopy and molecular modeling investigation of the binding of N-acetylneuraminic acid derivatives to rhesus rotavirus VP8* core. *Glycobiology.* 17:68–81.

Haselhorst T, Wilson JC, Thomson RJ, McAtamney S, Menting JG, Coppel RL, von Itzstein M. 2004. Saturation transfer difference (STD) 1H-NMR experiments and in silico docking experiments to probe the binding of N-acetylneuraminic acid and derivatives to Vibrio cholerae sialidase. *Proteins.* 56:346–353.

Hodsdon ME, Ponder JW, Cistola DP. 1996. The NMR solution structure of intestinal fatty acid-binding protein complexed with palmitate: Application of a novel distance geometry algorithm. *J Mol Biol.* 264:585–602.

Hua Y, Du Y, Yu G, Chu S. 2004. Synthesis and biological activities of octyl 2, 3-di-O-sulfo-alpha-L-fucopyranosyl-(1→3)-2-O-sulfo-alpha-L-fucopyranosyl-(1→4)-2, 3-di-O-sulfo-alpha-L-fucopyranosyl-(1→3)-2-O-sulfo-alpha-L-fucopyranosyl-(1→4)-2, 3-di-O-sulfo-beta-L-fucopyranoside. *Carbohydr Res.* 339:2083–2090.

Johnson BA, Blevins RA. 1994. NMRView: A computer program for the visualization and analysis of NMR data. *J Biomol NMR.* 4:603–614.

Kusaykin M, Bakunina I, Sova V, Ermakova S, Kuznetsova T, Besednova N, Zaporozhets T, Zvyagintseva T. 2008. Structure, biological activity, and enzymatic transformation of fucoidans from the brown seaweeds. *Biotechnol J.* 3:904–915.

Lake AC, Vassy R, Di Benedetto M, Lavigne D, Le Visage C, Perret GY, Letourneur D. 2006. Low molecular weight fucoidan increases VEGF165-induced endothelial cell migration by enhancing VEGF165 binding to VEGFR-2 and NRP1. *J Biol Chem.* 281:37844–37852.

Lamba D, Glover S, Mackie W, Rashid A, Sheldrick B, Perez S. 1994. Insights into stereochemical features of sulphated carbohydrates: X-Ray crystallographic and modelling investigations. *Glycobiology.* 4:151–163.

Lambris JD, Reid KB, Volanakis JE. 1999. The evolution, structure, biology and pathophysiology of complement. *Immunol Today.* 20:207–211.

Lee NY, Ermakova SP, Choi HK, Kusaykin MI, Shevchenko NM, Zvyagintseva TN, Choi HS. 2008. Fucoidan from Laminaria cichorioides inhibits AP-1 transactivation and cell transformation in the mouse epidermal JB6 cells. *Mol Carcinog.* 47:629–637.

Lii JH, Allinger NL. 1989a. Molecular mechanics. The MM3 force field for hydrocarbons. 3. The van der Waals' potentials and crystal data for aliphatic and aromatic hydrocarbons. *J Am Chem Soc.* 111:8576–8582.

Lii JH, Allinger NL. 1989b. Molecular mechanics. The MM3 force field for hydrocarbons. II: Vibrational frequencies and thermodynamics. *J Am Chem Soc.* 111:8566–8575.

Mabeau S, Kloareg B, Joseleau JP. 1990. Fractionation and analysis of fucans from brown algae. *Phytochemistry.* 29:2441–2445.

Mayer M, Meyer B. 1999. Characterization of ligand binding by saturation transfer difference NMR spectra. *Angew Chem Int Ed.* 35:1784–1788.

Mayer M, Meyer B. 2001. Group epitope mapping by saturation transfer difference NMR to identify segments of a ligand in direct contact with a protein receptor. *J Am Chem Soc.* 123:6108–6117.

Meyer B, Peters T. 2003. NMR spectroscopy techniques for screening and identifying ligand binding to protein receptors. *Angew Chem Int Ed Engl.* 42:864–890.

Mulloy B. 2005. The specificity of interactions between proteins and sulfated polysaccharides. *An Acad Bras Cienc.* 77:651–664.

Mulloy B, Gee C, Wheeler SF, Wait R, Gray E, Barrowcliffe TW. 1997. Molecular weight measurements of low molecular weight heparins by gel permeation chromatography. *Thromb Haemost.* 77:668–674.

Mulloy B, Mourao PA, Gray E. 2000. Structure/function studies of anticoagulant sulphated polysaccharides using NMR. *J Biotechnol.* 77:123–135.

Nardella A, Chaubet F, Boisson-Vidal C, Blondin C, Durand P, Jozefonvicz J. 1996. Anticoagulant low molecular weight fucans produced by radical process and ion exchange chromatography of high molecular weight fucans extracted from the brown seaweed Ascophyllum nodosum. *Carbohydr Res.* 289:201–208.

Skidmore MA, Guimond SE, Rudd TR, Fernig DG, Turnbull JE, Yates EA. 2008. The activities of heparan sulfate and its analogue heparin are dictated by biosynthesis, sequence, and conformation. *Connect Tissue Res.* 49:140–144.

Speth C, Wurzner R, Stoiber H, Dierich MP. 1999. The complement system: Pathophysiology and clinical relevance. *Wien Klin Wochenschr.* 111:378–391.

Tedesco F, Fischetti F, Pausa M, Dobrina A, Sim RB, Daha MR. 1999. Complement-endothelial cell interactions: Pathophysiological implications. *Mol Immunol.* 36:261–268.

Tissot B, Daniel R. 2003. Biological properties of sulfated fucans: The potent inhibiting activity of algal fucoidan against the human compliment system. *Glycobiology.* 13:29G–30G.

Tissot B, Gonnet F, Iborra A, Berthou C, Thielens N, Arlaud GJ, Daniel R. 2005. Mass spectrometry analysis of the oligomeric C1q protein reveals the B chain as the target of trypsin cleavage and interaction with fucoidan. *Biochemistry.* 44:2602–2609.

Tissot B, Montdargent B, Chevolot L, Varenne A, Descroix S, Gareil P, Daniel R. 2003. Interaction of fucoidan with the proteins of the complement classical pathway. *Biochim Biophys Acta.* 1651:5–16.

Usov AI, Bilan MI. 2009. Fucoidans - Sulfated polysaccharides of brown algae. *Russ Chem Rev.* 78:785–799.

Winkler M. 2001. Ancient proteins and futuristic surgery: The role of complement in discordant xenograft rejection. *Transplant Proc.* 33:3862–3864.